Applied Scientific Research **57**: 279–290, 1997.

Vortex Stretching and Filaments

PHILIPPE PETITJEANS and JOSÉ-EDUARDO WESFREID
Laboratoire de Physique et Mécanique des Milieux Hétérogènes, URA CNRS 857, Ecole Supérieure de Physique et de Chimie Industrielles (ESPCI), 10, rue Vauquelin, 75005 Paris, France

Received 30 August 1996; accepted in revised form 1 September 1997

Abstract. This paper presents a new technique to produce controlled stretched vortices. Intense elliptical vortices are created by stretching of an initial vorticity sheet. The initial vorticity comes from a laminar boundary layer flow and the stretching is parallel to the vorticity vectors. This low velocity flow enables direct observation of the formation and destabilization of vortices. Visualizations are combined with quasi-instantaneous measurements of a full velocity profile. The velocity profile is obtained with an ultrasonic pulsed Doppler velocimeter. The evolution of the central diameter of the vortices is related to the stretching. It is observed that destabilization occurs by pairing of two vortices, by hairpin deformation, and by breakdown of vortices into a "coil shape".

Key words: vortex, turbulence.

Introduction

A new technique is presented which produces stretched filamentary vortices in a controlled manner. The topic of vortex stretching is very interesting and relevant for a better understanding of fundamental mechanics in turbulence. Preliminary results illustrating the capabilities of this experiment are presented in this paper.

It has been shown numerically by Siggia [1] that the regions of largest vorticity concentration in a turbulent flow look like filaments. Other numerical simulations have confirmed these results [2–4]. Filaments have been observed in experiments by Cadot et al. [5] in a turbulent flow in a cylinder between two counter-rotating stirrers. The observed filaments corresponded to low pressure regions. They are generated by local stretching of the vorticity sheets [6]. Recall the three-dimensional vorticity equation:

$$\frac{\mathrm{d}\bar{\omega}}{\mathrm{d}t} = \frac{\partial\bar{\omega}}{\partial t} + (\bar{V}\cdot\nabla)\bar{\omega} = \nu\Delta\bar{\omega} + (\bar{\omega}\cdot\nabla)\bar{V},$$

where $\bar{V}$ is the velocity and $\bar{\omega} = \mathrm{rot}\,(\bar{V})$ is the vorticity. Enhancement of vorticity by stretching is represented by the last term of the equation.

Due to the turbulent character of such flows, it is difficult to study in detail the fundamental mechanisms that lead to the creation, evolution and destabilization of vorticity filaments. The problem of three-dimensional instabilities of vortex lines is still under theoretical investigation from the fundamental point of view [7–9].

This paper presents a new set-up to experimentally study the effects of stretching on a controlled vorticity sheet coming from a laminar boundary layer flow on a flat

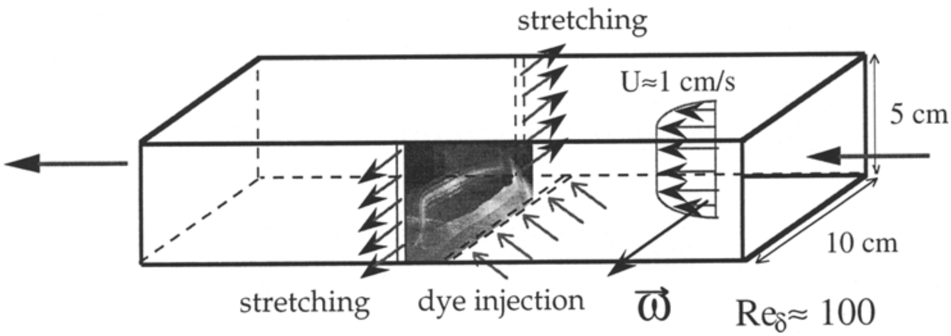

Figure 1. Experimental set-up.

plate. This flow is not turbulent. Therefore, the characteristic time and length scales are large enough so as to enable study of the instability. At the same time it provides a good model of vorticity instabilities occurring in fully turbulent flows. Thus, this experiment opens the possibility to accomplish quantitative measurements of the dispersion relation of vortex instabilities.

Experiments and Results

The key elements of the experimental set-up are presented in Figure 1. The rest of the set-up consists of a low-velocity water channel with very well-controlled flow. The flow is generated by a constant head pressure tank. A diffuser keeps the flow laminar with a minimum of perturbation. In the straight part (60 cm $\times$ 12 cm $\times$ 7 cm) (Figure 1), the flow develops a laminar boundary layer on each wall with a velocity of order 1 cm/s far away from the wall. The Reynolds number based on the boundary layer thickness is $\mathrm{Re}_\delta \approx 100$. The boundary layers on the lower and upper walls form the initial vorticity, $\boldsymbol{\omega} = \pm\omega\mathbf{z}$. The vorticity sheet is stretched parallel to the vorticity vector by means of a flow slot on each lateral wall (Figure 1). The total flow rate through the channel is controlled as well as the flow rate in the flow slots; consequently, the initial vorticity can be controlled (via the thickness of the boundary layer) as well as the stretching. For a given flow rate, the formation of periodic vortices by roll-up of fluid sheets is obtained when the stretching is larger than a threshold. Figure 2 presents the threshold of the mean stretching rate, γ, above which vortices are emitted periodically, as a function of an estimate of the initial vorticity ω_i. The mean stretching rate γ is evaluated by assuming that the stretching velocity is zero in the middle of the length of the vortices (symmetry): $\gamma \approx U_s/l$ where U_s is the mean velocity in the slots, and l is half the width of the channel (6 cm). The initial vorticity ω_i is estimated from the velocity U_0 in the center of the channel and the thickness of the boundary layer δ: $\delta = (L\nu/U_0)^{1/2} = L/(\mathrm{Re})^{1/2}$, where L is the entrance length, and ν the kinematic viscosity. The initial vorticity is then $\omega_i \approx U_0/\delta$. These are estimates which we will make quantitatively precise in the future.

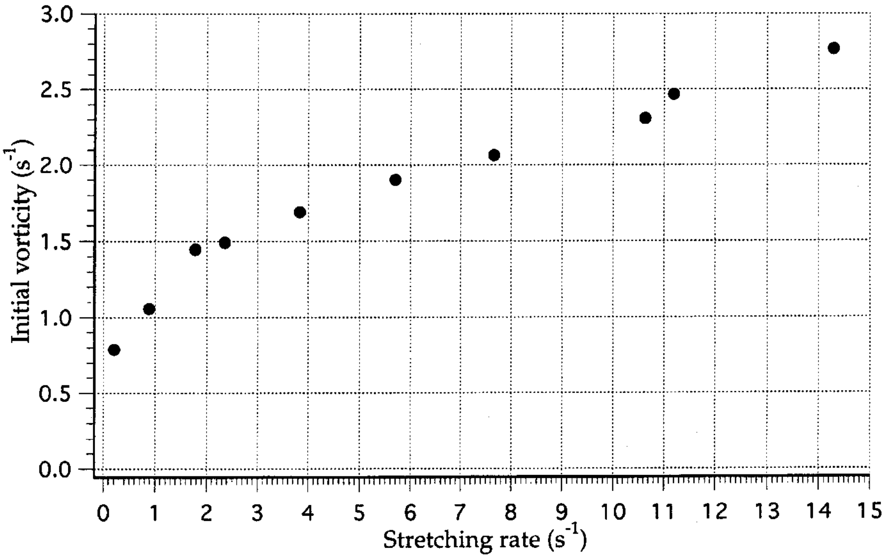

Figure 2. Threshold of the mean stretching rate γ above which vortices are emitted periodically, as a function of the initial vorticity ω_i.

The formation, development and destabilization of these vortices is visualized by injection of a sheet of fluorescent dye (fluoresceine) on the wall, 2 cm upstream from the stretching position (Figure 1). The dye is injected into a thin transverse slot (1 mm thick and is inclined at 30 degrees with respect to the bottom). An argon laser beam, expanded by passing through two mutually perpendicular cylindrical lenses, is used to fluoresce the dye, permitting the visualization of the formation of the rolls. Figure 3 shows such a visualization. The dye sheet separates from the injector, and penetrates into the vortex by winding around the axis. Because of a low molecular diffusion coefficient, ($D \approx 3.6 \times 10^{-6}$ cm^2/s) it is possible to distinguish several layers of dye turning around the axis of the vortex in a helical way (Figure 3). A very thin dye filament is observed that shows the axis of the vortex. Then, the dye is removed to the two sides towards the slots on the lateral walls of the channel, which shows that the stretching velocity only occurs at the core of the vortex. Another vortex is then generated, and so on, with a periodicity due to the permanent longitudinal flow.

We get the fully quasi-instantaneous vertical velocity profile, $v(y)$ with an Ultrasonic Doppler Velocimeter (UDV), DOP 1000. The DOP 1000* is an Ultrasonic Pulsed Doppler Multigate Velocimeter that measures a velocity component profile along the transducer axis. The transducer generates a pulse wave that propagates as a thin acoustic beam, representing the global measurement volume. The maximum measurement depth, $P_{\max}$, is determined by the repetition frequency of the pulses

* Manufactured by Signal Processing S.A.

Figure 3a. Visualization of a vortex created by stretching. The view corresponds to the position of Figure 1.

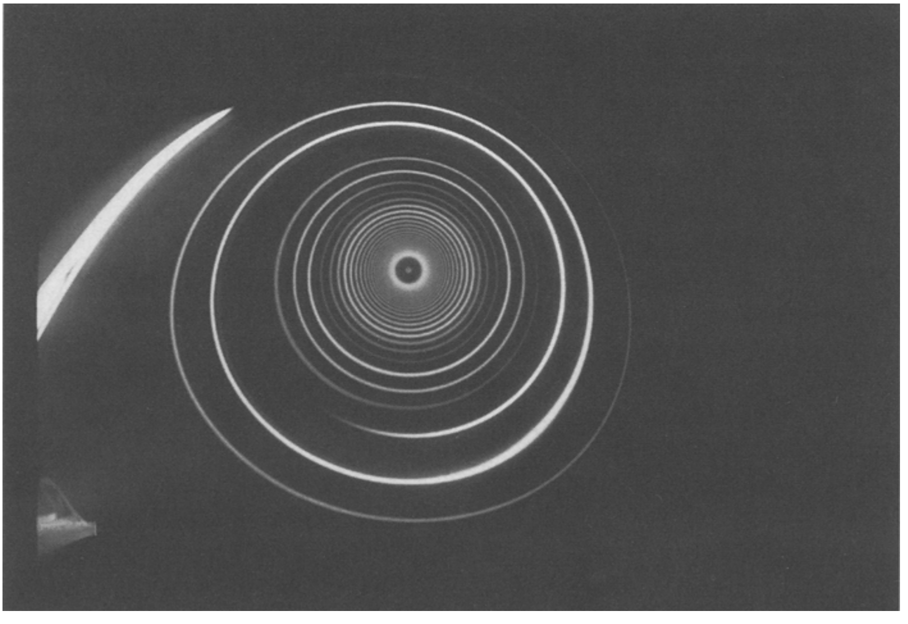

Figure 3b. Cross section of a stretched vortex. The dye sheet penetrates into the vortex by winding around its axis.

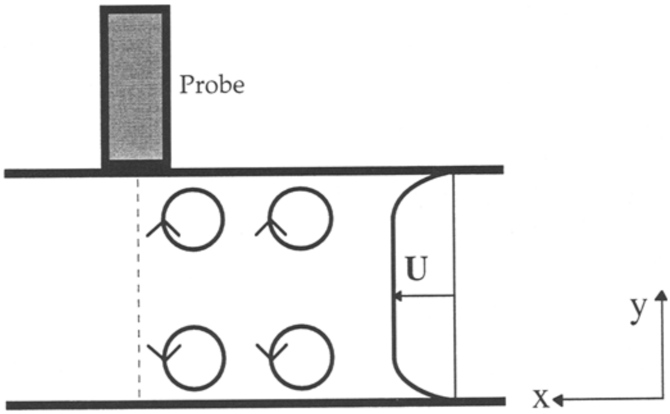

Figure 4. Schematic view of the position of the probe and vortices.

(f_{PRF}), which has the relation: $P_{\max} = c/(2f_{\mathrm{PRF}})$ where c is the speed of sound. The typical value of f_{PRF} used in the experiment was 976 Hz. This gives a $P_{\max}$ value of 77 cm. This depth can be divided by 2, 4 or 8 to increase the spatial resolution. Since the sound speed in the water is constant $c = 1500$ m/s, the time delay between two pulses represents both the outgoing and the incoming distance covered by the pulse wave. Every particle of suitable diameter going across this beam will produce an echo collected by the transducer (one transducer is used in backscatter mode), and analyzed by the multigate processor of the UDV. Two measurements are extracted from the echo signal: the Doppler frequency (to obtain the probe-axis component of the velocity), and the time delay between the emission of the pulse and the subsequent echo (to obtain the position along the transducer axis). A maximum of 220 positions along the measurement range can be obtained. Thus, every block of data between the two pulses produces a velocity profile. It is possible to build velocity profiles using between 16 and 512 pulses. This gives the time step range between two full profiles of 0.03 and 1.05 s, respectively. The probe is positionned as indicated in Figure 4 and measures the velocity profile, $v_i(y)$, as a function of time. In this experiment, the time step between two profiles of 114 points is $\Delta T = 0.12$ s. This produces a $v(y,t)$ dataset that can be visualized as an image with image analysis software* which builds an image where the velocities are linearly scaled between 0 and 255 (in grayscale). The data is processed with a median image filter for noise reduction. The advantage of using this filter on the image instead of on the initial data, is that the filter reduces noise by taking into account both velocities forward and backward in time as well as space. Two examples of what is obtained are given in Figure 5 where a double array of vortices on the upper and lower walls are observed. The centers of the (lower)

* NIH Image freeware software, from the National Inst. of Health, avalaible via ftp at zippy.nimh.nih.gov.

vortices are located at $y^* = 0.75$ cm from the bottom. At this given position of y^*, the Reynolds numbers, $\mathrm{Re} = Uy^*/\nu$, in the two experiments, are $\mathrm{Re} = 61$ and $\mathrm{Re} = 4.7$, respectively. Only the lower array is visualized since dye is injected only on the lower wall, but it is clear that there is an equivalent vorticity sheet on the upper wall which is also stretched due to the slots constituting the full height of the lateral walls (Figure 1). The vorticity in the array of vortices on the lower wall is larger than that on the upper wall because of the injection of dye on this wall, which enhances the initial shear. The vortices are emitted regularly and in these examples, the frequencies of emission are respectively, $f = 0.134$ Hz and $f = 0.050$ Hz. Vortices on the upper and the lower walls are emitted in phase. It is possible to compare vortices generated by this flow with those generated in other flows such as wakes and jets. Indeed, when jets or bodies in wakes are close to each other, the vortices are in phase opposition. When the distance between them is larger, vortices are in phase. The same mecanisms might also act in our case: if the distance between the vortices is large (large height of the channel), then vortices are emitted in phase. For a smaller distance, vortices would be emitted in phase opposition. In our apparatus, it is not possible to change the distance between the walls to verify the validity of this explanation.

The spatial size of the vortices is estimated by the transformation, $x = U_a(y^*) \cdot T$, where $U_a(y^*)$ is the advection velocity of the frozen vortices (which is of the same order as U). The spatial step, at y^*, is $\Delta x = U_a \cdot \Delta T \approx 0.083$ cm in the first case of Figure 5, and $\Delta x \approx 0.007$ cm in the second case. From this the central diameter Φ of the vortex corresponding to the distance between the two maxima of vertical velocity at the center is obtained (Figures 5 and 6).

This size is measured as a function of the stretching velocity, U_s. This velocity, defined as the mean velocity in the slots, is obtained from the flow-rate which is measured. Although the relevant parameter should be the velocity gradient in the axis of the vortex, it is not used because this parameter has been unable to be accessed yet. For the same flow, the core diameter is measured for eight different values of the stretching velocity, U_s, between 39 and 94 cm/s. In that case, the diameters of the vortices are between 3.75 and 1.25 cm. Figure 7 presents the central diameter, Φ, of the vortex and its amplitude as a function of the stretching velocity, V. The central diameter decreases with the stretching velocity, while its intensity increases. This is qualitatively similar to what happens in a Burgers' vortex which approximates our stretched vortices.

It is deduced from Figure 5 and from the fact that $U_a = U_a(y)$, that the circular cross-section of vortices is deformed (elliptical form) and is tilted (Figure 6). This is due to the fact that the advection velocity still has a boundary layer profile due to the wall. The closer the flow is to the wall, the lower the advection velocity. To the contrary, the flow far away from the walls has a larger velocity, so that the part of a vortex in this region is advected faster than the lower part, which produces this deformation and inclines the roll. This mechanism is also responsible for the vortex pairing instability [11] that is observed very clearly in this experiment

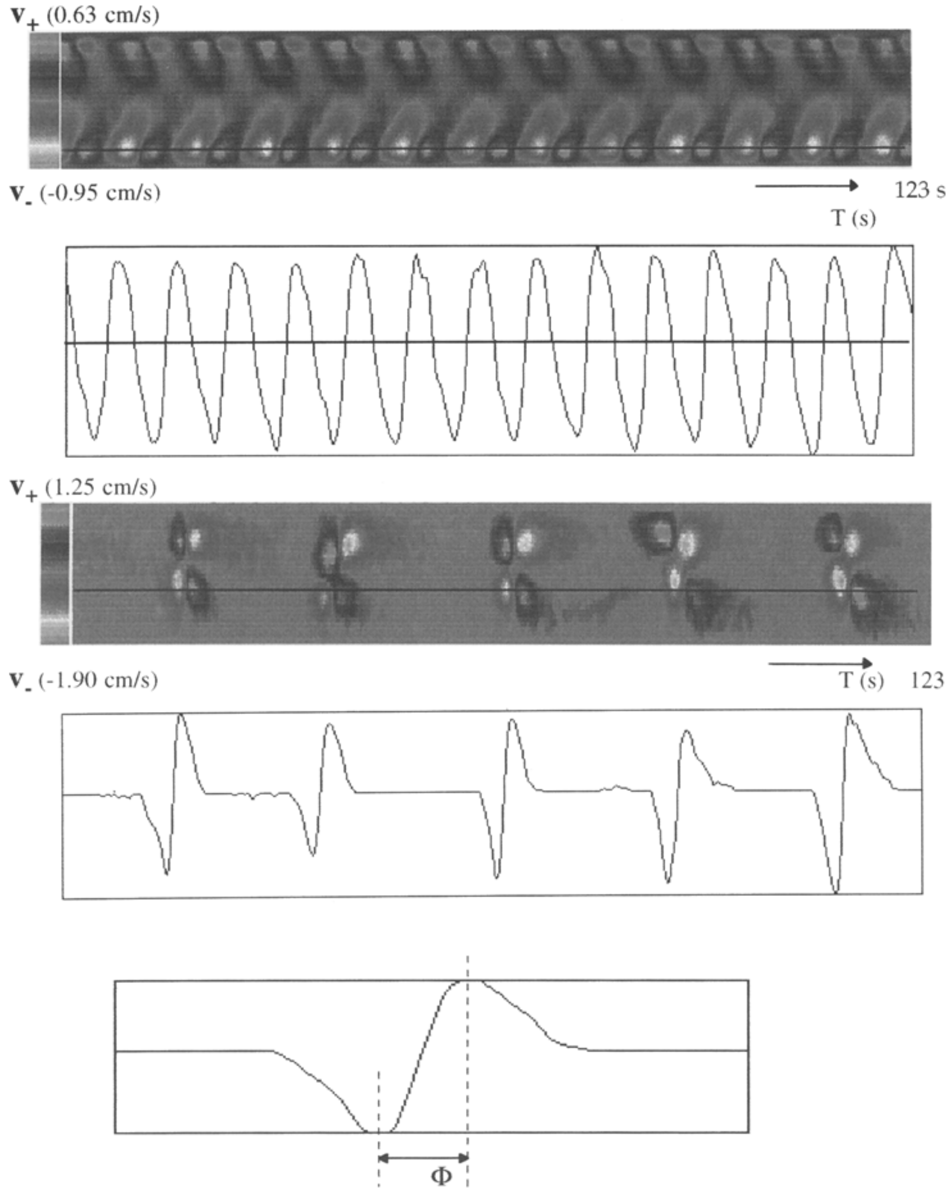

Figure 5. Two examples of the vertical velocity as a function of time from 0 to 123 s. A slice along the black line in of these images gives the evolution of the vertical velocity with time at the position y^* where the centers of the vortices are located. The last drawing shows how the central diameter is measured (see also Figure 6).

(Figure 8). A perturbation of the fastest moving part of a vortex (farthest from the wall) catches up with the slowest moving part of the preceding vortex. This is seen in the observations that the two vortices first rotate around each other, and then

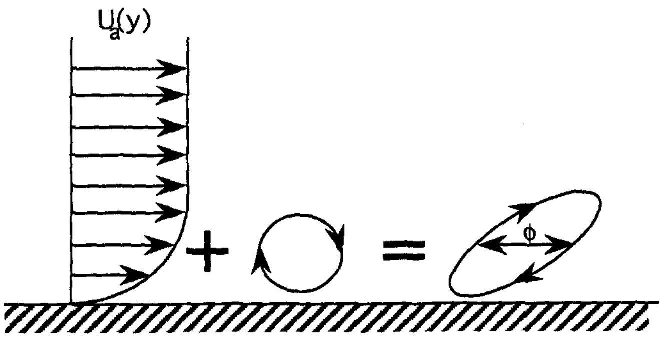

Figure 6. A schematic illustration of the elliptical form of the vortices due to the boundary layer velocity profile.

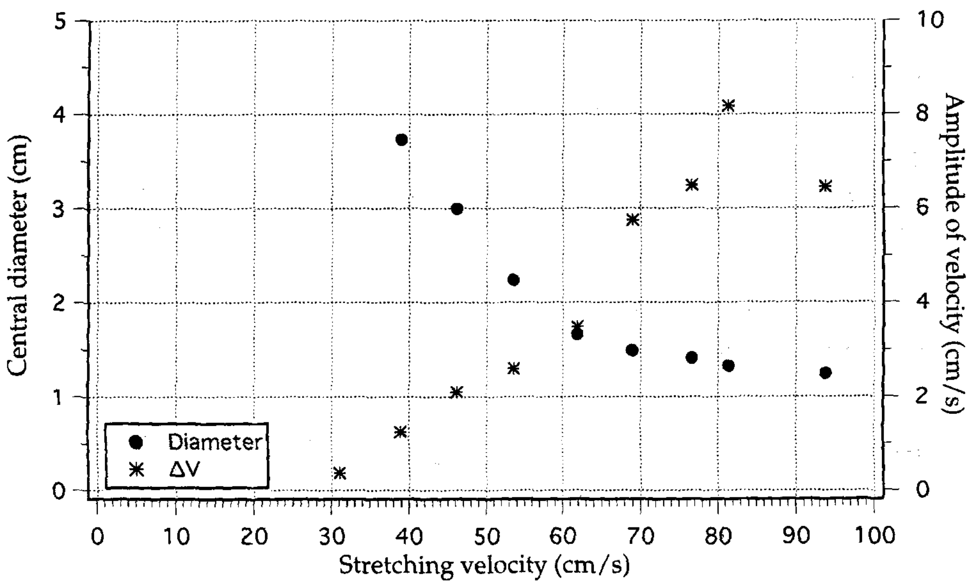

Figure 7. Evolution of the central diameter and the vertical velocity amplitude of vortices as a function of the stretching velocity.

coalesce into a stronger vortex. This instability can be controlled by means of the advection velocity.

Another observed instability concerns the sinuous deformation of the vortex. The transversal perturbation is amplified by the difference in vertical velocities and this produces a localized longitudinal line (hairpin). This effect is magnified by the attachment of the vortex to the slots on the walls.

The last instability observed is a "vortex breakdown" instability [12]. We observe that this instability happens when a type of solitary wave propagates along the vortex (Figure 9) producing a loss of its axial symmetry. The vortex deforms in a

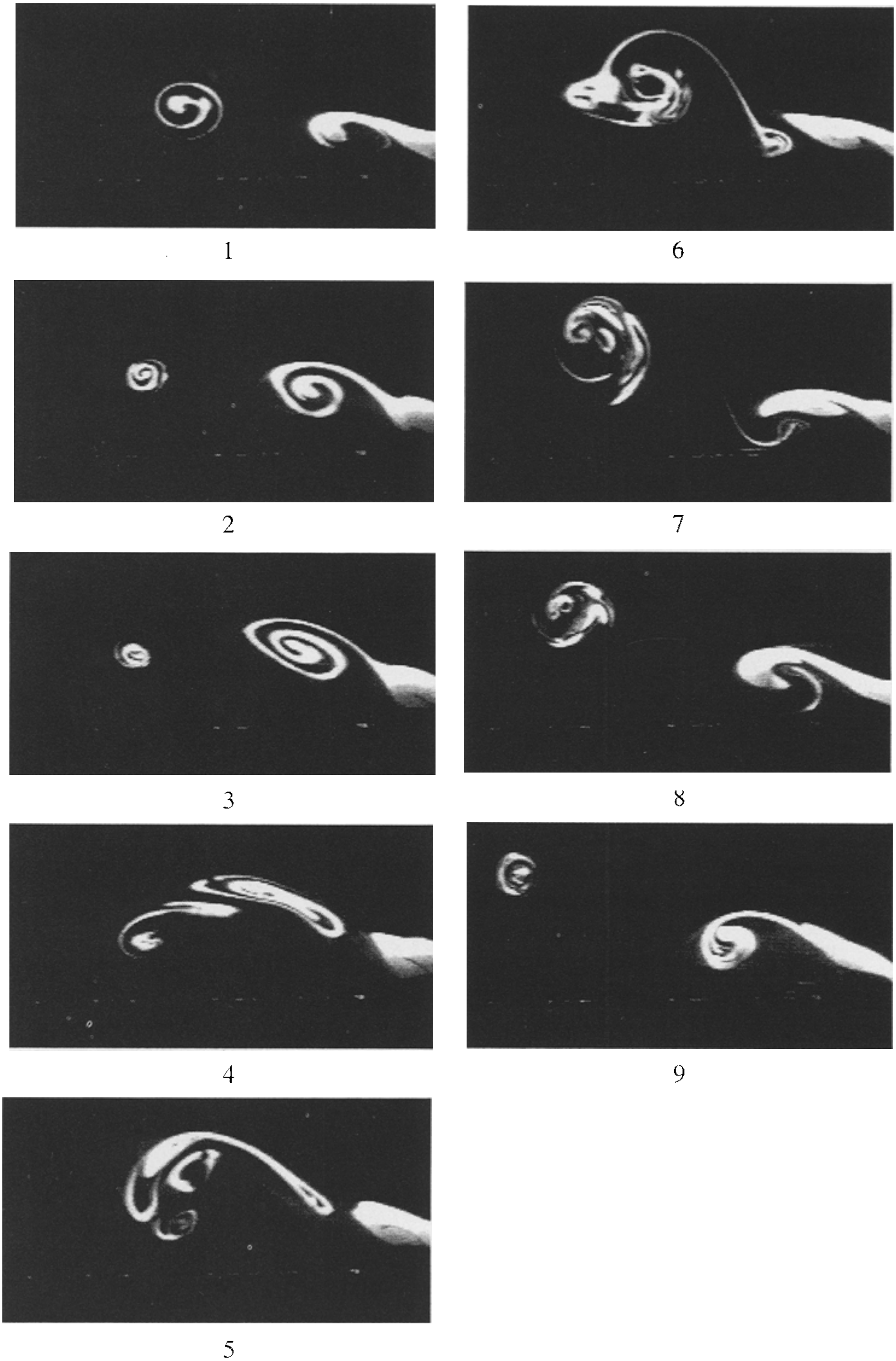

Figure 8. A sequence of 8 views during 3 seconds showing the pairing of two vortices.

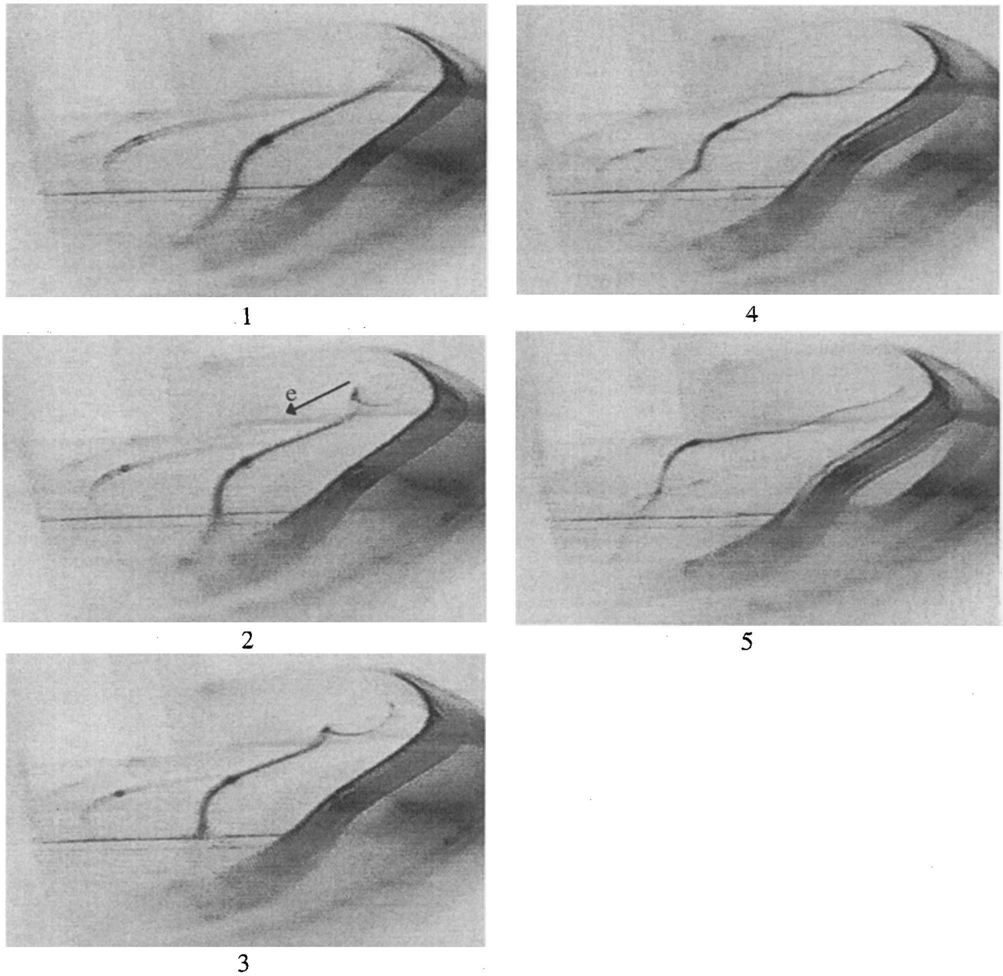

Figure 9. A sequence of 5 views during 4 seconds showing the propagation of a wave along the filament. The velocity of the wave is $e \approx 1.6$ cm/s.

helical fashion and collapses into a "coil shape" as a turbulent spot (Figure 10). This transition is clearly observed in this experiment and gives a picture of some intermittent features of turbulent flows.

Experiments are in progress which will characterize the region of parameters (flow velocity and stretching) where these instabilities occur.

Conclusion

The main point of this preliminary work is the design of an experimental set-up which enables direct observation of the dynamics of vortices under stretching, and gives direct access to the fundamental mechanisms which play a role in this

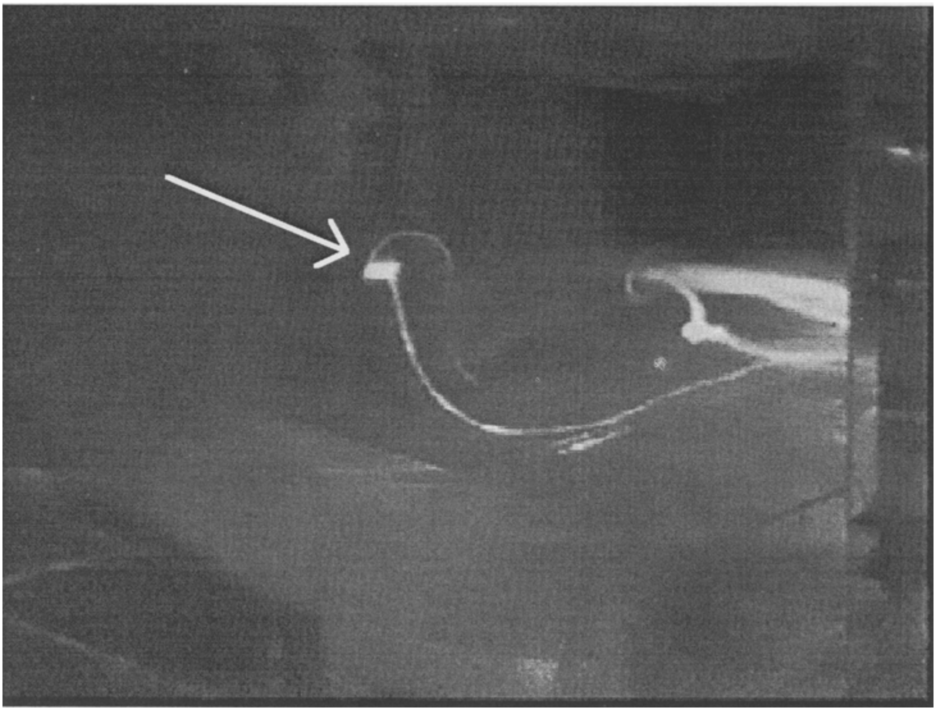

Figure 10. View of a turbulent spot during the breakdown of a vortex.

problem. These experiments clearly show the formation of vortices by a rolling-up. type mechanism The diameter and amplitude of the vortices are related to the stretching. The measured velocity profile shows the existence of a double array of vortices near the upper and lower wall. This confirms that vortices are not created by deformation of the boundary layer by the dye injection(as is the case observed by [13] with an injection through the wall).

Several forms of destabilization are observed by pairing, by sinuous deformation, or by breakdown. Details of the intermittent "coil shape" transition are seen as the ultimate evolution of vortex breakdown. Shear and velocity profiles deform the vortex in an elliptical manner. As it is known from the inviscid theory of stability, elliptical vortices can produce three-dimensional instabilities similar to what is observed in these experiments.

Work is now in progress, in a new facility, fully devoted to take advantage of this new technique of vortex stretching, in order to systematically study the stability of these structures.

Acknowledgments

Thanks are due to M.E. Brachet for interesting discussions, and M. Michaelian for help in proof reading.

References

1. Siggia, E.D., Numerical study of small-scale intermittency in three-dimensional turbulence. *J. Fluids Mech.* **107** (1981) 375–406.
2. Brachet, M.E., Meneguzzi, M., Vincent, A., Politano, H. and Sulem, P.L., Numerical evidence of smooth self-similar dynamics and possibility of subsequent collapse for three-dimensional ideal flows. *Phys. Fluids A* **4**(12) (1992) 2845–2854.
3. Passot, T., Politano, H., Sulem, P.L., Angilella, J.R. and Meneguzzi, M., Instability of strained vortex layers and vortex tube formation in homogeneous turbulence. *J. Fluid Mech.* **282** (1995) 313–338.
4. Jiménez, J., Wray, A.A., Saffman, P.G. and Rogallo, R.S., The structure of intense vorticity in homogeneous isotropic turbulence. *J. Fluid Mech.* **255** (1993) 65–90.
5. Cadot, O., Douady, S. and Couder, Y., Characterization of the low pressure filaments in three-dimensional turbulent shear flow. *Phys. Fluids.* **7**(3) (1995) 630–646.
6. Neu, J.C., The dynamics of stretched vortices. *J. Fluid Mech.* **143** (1984) 253–276.
7. Moffatt, H.K., Kida, S. and Ohkitani, K., Stretched vortices – The sinews of turbulence; Large-Reynolds-number asymptotics. *J. Fluid Mech.* **259** (1994) 241–264.
8. Bayly, B., Three-dimensional instability of elliptical flow. *Phys. Rev. Lett.* **57** (1986) 2160–2163.
9. Le Dizès, S., Rossi, M. and Moffatt, H.K., On three-dimensional instability of elliptical vortex subjected to stretching. *Phys. Fluids* **8**(8) (1996) 2084–2090.
10. Burgers, J.M., A mathematical model illustrating the theory of turbulence. *Adv. Appl. Mech.* **1** (1948) 171–199.
11. Saffman, P.G. and Baker, G.R., Vortex interactions. *Ann. Rev. Fluid Mech.* **11** (1979) 95–122.
12. Hall, M.G., Vortex breakdown. *Ann. Rev. Fluid Mech.* **4** (1972) 195–218.
13. Acarlar, M.S. and Smith, C.R., A study of hairpin vortices in laminar boundary layer. Part 2. Hairpin vortices generated by fluid injection. *J. Fluid Mech.* **175** (1987) 43–84.